

混凝土外加剂及其应用技术论坛2019年会

2019



聚羧酸系高性能减水剂及其 应用技术新进展—2019

*Recent Advances in Polycarboxylate Superplasticizer and
Application Technology-2019*

混凝土外加剂及其应用技术论坛 编

 **北京理工大学出版社**
BEIJING INSTITUTE OF TECHNOLOGY PRESS



聚羧酸系高性能减水剂及其 应用技术新进展—2019

混凝土外加剂及其应用技术论坛 编

 **北京理工大学出版社**
BEIJING INSTITUTE OF TECHNOLOGY PRESS

版权专有 侵权必究

图书在版编目 (CIP) 数据

聚羧酸系高性能减水剂及其应用技术新进展. 2019/混凝土外加剂及其应用技术论坛编. —北京: 北京理工大学出版社, 2019. 3

ISBN 978 - 7 - 5682 - 6829 - 5

I. ①聚… II. ①混… III. ①混凝土 - 减水剂 - 文集 IV. ①TU528.042.2 - 53

中国版本图书馆 CIP 数据核字 (2019) 第 043057 号

出版发行 / 北京理工大学出版社有限责任公司

社 址 / 北京市海淀区中关村南大街 5 号

邮 编 / 100081

电 话 / (010) 68914775 (总编室)

(010) 82562903 (教材售后服务热线)

(010) 68948351 (其他图书服务热线)

网 址 / <http://www.bitpress.com.cn>

经 销 / 全国各地新华书店

印 刷 /

开 本 / 787 毫米 × 1092 毫米 1/16

印 张 / 39

字 数 / 916 千字

版 次 / 2019 年 3 月第 1 版 2019 年 3 月第 1 次印刷

定 价 / 169.00 元

责任编辑 / 王玲玲

文案编辑 / 王玲玲

责任校对 / 周瑞红

责任印制 / 李志强

图书出现印装质量问题, 请拨打售后服务热线, 本社负责调换

前 言

聚羧酸系高性能减水剂是一种新型、绿色环保的高性能减水剂，与传统减水剂相比，其具有分散性强、减水率高、混凝土的坍落度经时间损失小等显著的综合技术优势，对提高混凝土性能、保证工程质量发挥了十分重要的作用，成为国家重点、重大工程中首选外加剂，其使用量持续快速增长。随着聚羧酸系高性能减水剂及其应用技术的不断发展，相继出现了早强型、缓凝型、缓释型、防冻型和减缩型等功能性聚羧酸系高性能减水剂，满足了混凝土施工及工程应用的需要。

为了更好地总结聚羧酸系高性能减水剂的国内外研究成果与其工程应用经验，促进聚羧酸系高性能减水剂研究的技术创新和技术发展，进一步推动聚羧酸系高性能减水剂及其应用技术的可持续性发展，2019年4月24—26日在重庆举办“第七届聚羧酸系高性能减水剂及其应用技术交流会”暨“混凝土外加剂及其应用技术论坛2019年会”。

本次会议征集到学术论文100余篇，经会议学术委员会专家审核，择录了97篇论文，经编辑正式出版名为《聚羧酸系高性能减水剂及其应用技术新进展—2019》的论文集。本论文集内容涉及聚羧酸系高性能减水剂国内外研究进展与发展趋势、理论研究、最新制备技术、在各类水泥混凝土制品与工程中应用技术新进展及其案例分析、相关检测及标准；聚羧酸系高性能减水剂用功能性材料的理论研究与应用技术；其他混凝土外加剂的应用技术及机理研究等。论文集学术水平较高、内容较丰富、涉及面较广，具有一定学术参考价值，为读者提供了大量的技术资料。

由于时间与水平有限，论文集中难免有不妥之处，敬请读者予以指正。

混凝土外加剂及其应用技术论坛
2019年3月

目 录

综述与基础理论

1. Non - Classical Nucleation Mechanism of C - S - H	3
2. C - S - H 非经典成核机理	11
3. 聚羧酸减水剂在碱激发矿渣体系中分散性能的研究	18
4. 混凝土坍落度保持剂的研究	24
5. Na^+ 和 Ca^{2+} 对聚羧酸分子溶液构象的影响	30
6. 基于随机次序吸附模型的聚羧酸吸附动力学分析	37
7. 三种含氧官能团在 CaCO_3 表面的吸附模拟	44
8. 低表面张力聚羧酸减水剂对水泥基材料的减缩作用研究	50
9. 滴加工工艺对聚羧酸合成的影响	57
10. 降粘型聚羧酸减水剂的制备及其性能研究	64
11. 聚乙二醇乙基醚稳定性研究	71
12. 聚羧酸减水剂与水泥浆体流变参数的相关性分析	77
13. 抗泥型聚羧酸高性能减水剂制备与性能研究	85
14. 不同酸醚比的聚羧酸减水剂在水溶液中的构象变化	93

复配与应用技术

15. 基于轨道交通自密实混凝土工程外加剂的研究应用	101
16. Study on the Performance of The Low Temperature Cementitious Grout for Reinforcement Couplers	108
17. 聚羧酸系高性能减水剂的智能生产系统设计与实现	114
18. 智能控制一体化系统在聚羧酸减水剂生产中应用与发展现状	120
19. 聚羧酸系减水剂与机制砂石粉的相容性研究	127
20. 聚羧酸减水剂在机制砂配置管桩泵送混凝土中的应用	133
21. 一种乙基醚保坍型减水剂的合成和应用	139
22. 酯醚共聚型聚羧酸减水剂敏感性及工程应用研究	143
23. 聚羧酸减水剂与木质素磺酸钠复配对混凝土性能的影响	151
24. 葡萄糖酸钠与聚羧酸减水剂在水泥表面竞争吸附的研究	158
25. PCE 在沪通长江大桥超高主塔混凝土中的应用	163
26. 聚羧酸减水剂复配有有机醇胺类防冻剂的试验研究	169
27. 缓释型 PCE 在岩溶地区超长灌注桩混凝土中的应用	175
28. 聚羧酸减水剂在“三低一高”混凝土中的应用	180

29. 一种新型聚羧酸系高性能减水剂的制备技术研究	187
30. 聚羧酸调节剂与机制砂混凝土适应性研究	193
31. 早强复合型聚羧酸减水剂在 PC 构件的应用研究	200
32. 聚羧酸减水剂腐败变质的影响因素研究	206
33. 粘土矿物对不同品种减水剂应用效果的影响研究	211
34. 低温条件下聚羧酸系高性能减水剂的工程应用	218
35. 缓释型聚羧酸减水剂在低坍落度混凝土中的应用	223

制备与性能研究

36. 甲基烯丙基聚氧乙烯醚衍生物的制备及其性能研究	231
37. 一种高适应性聚羧酸系减水剂的合成与性能研究	238
38. 低敏感型混凝土和易性调节剂的制备与性能研究	247
39. 超早强型聚羧酸减水剂的制备及其性能机理研究	253
40. 新型小分子减水剂的合成与性能研究	260
41. 一种缓凝型减水剂的制备及性能研究	267
42. 一种保坍型固体聚羧酸减水剂的制备工艺与性能研究	273
43. 降粘型聚羧酸高性能减水剂性能研究	282
44. 一种石粉适应型保坍剂的合成与性能表征	288
45. 一种缓凝型酯类减水剂合成与应用	294
46. 基于原子转移自由基聚合制备聚羧酸减水剂的研究	299
47. 抗泥保坍型聚羧酸系高性能减水剂的合成及性能研究	305
48. 含苯基建筑外加剂的合成与应用	315
49. 低敏感高适应性聚羧酸减水剂的合成与性能研究	320
50. 不同主链聚合度早强型聚羧酸减水剂的合成与表征	327
51. 酯化改性抗泥型聚羧酸减水剂的制备及其应用	335
52. 一种改性柠檬酸聚羧酸减水剂的合成研究	340
53. 一种保坍型聚羧酸减水剂的合成与性能研究	345
54. 聚醚相对分子质量对早强性能影响的研究	350
55. 引入磷酸基团的聚羧酸类减水剂的合成及性能	353
56. 超早强型聚羧酸减水剂聚醚的性能研究	359
57. VPEG 型聚羧酸减水剂的工艺研究	364
58. 高温适应性聚羧酸系减水剂的合成研究	371
59. 硅烷偶联剂改性聚羧酸保坍剂的制备与应用	378
60. 乙二醇单乙烯基聚乙二醇大单体 (EPEG) 合成聚羧酸减水剂的研究	384
61. 一种高性价比新型聚醚的性能研究	389
62. β -环糊精改性聚羧酸减水剂的制备与抗泥性能研究	399
63. 高保水型聚羧酸减水剂的制备及性能研究	405
64. 一种适用于机制砂混凝土的聚羧酸减水剂的制备	413
65. 一种抗泥型聚羧酸系高性能减水剂的制备及性能研究	417

66. 一种本体聚合聚羧酸系高性能减水剂的合成及性能研究	423
67. 不同酸醚比、MCH 用量对聚羧酸减水剂性能的影响研究	430
68. 一种缓释型聚羧酸高性能减水剂的制备及其性能研究	435

其他相关主题

69. 物理凝胶改性无碱速凝剂的制备与性能影响	443
70. 不同氟化物制备液体速凝剂及其性能对比研究	448
71. 新型液体无碱速凝剂的合成工艺参数探讨及适应性能研究	454
72. 中美混凝土外加剂标准对比	460
73. 聚羧酸型混凝土引气剂的试验研究	470
74. 一种混凝土保水剂的合成与性能评价	475
75. 碳酸钙微晶的制备及早强性能研究	480
76. 一种铁路压浆料抗折剂的研发与应用	485
77. 复配羧酸防腐理念	492
78. 三萜皂甙引气剂的复合改性研究	497
79. 生态混凝土外加剂的水泥适应性研究	503
80. 新型降粘型外加剂在建筑施工中的应用	508
81. 一种无碱液体速凝剂的制备及性能研究	513
82. 一种混凝土用和易性改进剂的应用研究	519
83. 复合型早强剂在构件混凝土中的应用研究	524
84. 机制砂级配对混凝土强度的影响	528
85. 自密实混凝土用粘度改性材料的复配及其性能研究	534
86. 一种新颖的聚醚类混凝土引气剂的制备及性能研究	540
87. 聚羧酸减水剂与不同缓凝剂复配性能评价	546
88. G25 - S3 混凝土保坍剂的制备及性能研究	552
89. 不同物质调整聚羧酸减水剂酸碱度对其性能影响的探讨	558
90. 衬砌管片表观质量影响因素探析	562
91. 脱硝粉煤灰对掺聚羧酸减水剂混凝土性能的影响研究	570
92. 生物多糖乳液对聚羧酸敏感性的抑制作用研究	576
93. 混凝土墙体局部外观异常质量可追溯性分析	581
94. Effect of Processing Conditions on Particle Size and Stability of C - S - H/PCE Nanocomposites	586
95. 焦亚硫酸钠 - 过硫酸铵引发体系合成聚羧酸减水剂	597
96. 不同偶氮引发剂对固体聚羧酸系减水剂性能的影响	603
97. Bleeding Property of the Fresh Cement Pastes Mixed with Polycarboxylate (PCE) Superplasticizers; an NMR Study	609

综述与基础理论

Non – Classical Nucleation Mechanism of C – S – H

Prof. Johann Plank

(Chair for Construction Chemistry, Technische Universität München)

ABSTRACT: Calcium silicate hydrate (C – S – H) presents the main component in hardened cement and is responsible for its principle properties such as compressive strength, brittleness etc. Currently, its formation is thought to start with nanofoils which then grow into the larger, well – known needles. Here, the early nucleation and crystallization of C – S – H precipitated from aqueous solutions of $\text{Ca}(\text{NO}_3)_2$ and Na_2SiO_3 was investigated. It was found that in the absence of PCE, globular nanoparticles of C – S – H with a diameter of ~ 50 nm are observed. Thereafter, within an hour the globules completely convert to the well – known nanofoils of C – S – H with ~ 150 nm length following a non – classical nucleation mechanism. In the presence of a PCE copolymer, the initial globules show a core – shell morphology, presumably with PCE polymer as shell (thickness 4 – 8 nm) which delays the conversion to the nanofoils for several hours. Apparently, the PCE layer effectively shields the C – S – H droplets and strongly delays transformation from the C – S – H globules to the nanofoils. ^{29}Si MAS NMR spectroscopy revealed that in the C – S – H globules, the silicate chains are slightly branched (Q^1 , Q^2 , Q^3 species) whereas in the C – S – H nanofoils only chains of silicate (Q^1 , Q^2 species) occur.

1 INTRODUCTION

Calcium silicate hydrate or C – S – H presents the main hydration product of ordinary Portland cement. C – S – H is generated from the hydration of the tricalcium silicate (C_3S) and dicalcium silicate (C_2S) phases via a dissolution – precipitation mechanism. It presents the binding phase which is responsible for the strength properties and durability in hardened cement. Generally, C – S – H exhibits low crystallinity and in hardened cement typically exhibits a Ca/Si molar ratio of 1.6 – 1.8. The layered structure of C – S – H consists of linear silicate chains which are aligned in “dreierketten” sequences and share oxygen atoms with calcium ions in plane.

The nucleation and crystallization of inorganic minerals is described by two theories. The first, classical nucleation theory is based on the formation and growth of nuclei. The second, non – classical nucleation concept presents that the morphology of the precritical clusters can differ significantly from that of the final bulk crystal. There, an amorphous intermediate (e. g. liquid droplets, amorphous nanoparticles) subsequently crystallizes to form the stable crystalline product.

Polycarboxylate (PCE) superplasticizers are known as high range water reducing admixtures

for concrete. PCEs improve the rheology via an electrosteric dispersing effect. The structure of anionic comb-like PCE copolymers consists of carboxylate anchor groups at the backbone which are negatively charged and responsible for the adsorption onto the positively charged surface sites of cement particles and hydration products like ettringite. While the non-ionic side chains of PCEs are made from polyethylene glycol (PEG) which is accountable for the dispersing ability via a steric hindrance effect.

Synthetic C-S-H-PCE nanocomposites are well-known seeding materials which can enhance the early strength of Portland cement and blended cements. They consist of C-S-H nanofoils which are stabilized by PCE copolymers adsorbed onto the positively charged surfaces of C-S-H. An ultra-small size of the C-S-H seeds is required to achieve a maximum seeding effect on cement hydration and consequently, a much enhanced early strength development of concrete. However, the initial nucleation and crystallization of C-S-H in the presence of PCE is still not well understood.

In this study, the very early nucleation and subsequent crystallization of C-S-H (5 min - 48 h) precipitated from $\text{Ca}(\text{NO}_3)_2$ and Na_2SiO_3 solutions at a Ca/Si ratio of 1.0 in the absence and presence of low and high concentrations of an IPEG-PCE superplasticizer was investigated by capturing the initial precursors of C-S-H via transmission electron microscopy (TEM). Additionally, their nanostructures were characterized via XRD and ^{29}Si MAS NMR spectroscopy.

2 Materials and Methods

2.1 Raw materials

The starting materials used in the synthesis of C-S-H were $\text{Ca}(\text{NO}_3)_2 \cdot 4\text{H}_2\text{O}$ (PanReac AppliChem, Germany) and $\text{Na}_2\text{SiO}_3 \cdot 5\text{H}_2\text{O}$ (VWR Prolabo BDH Chemicals, Germany). As PCE superplasticizer, a commercial isoprenyl oxy poly(ethylene glycol) based superplasticizer (IPEG PCE) (Sunrise Co., Ltd., Shanghai, China) was employed in the synthesis and its solid content was 40% by weight. The chemical structure of this PCE polymer is presented in Fig. 1 and its molecular properties and anionic charge amount are listed in Table 1. The pH value of the PCE solution was adjusted by using NaOH (Merck KGaA, Germany).

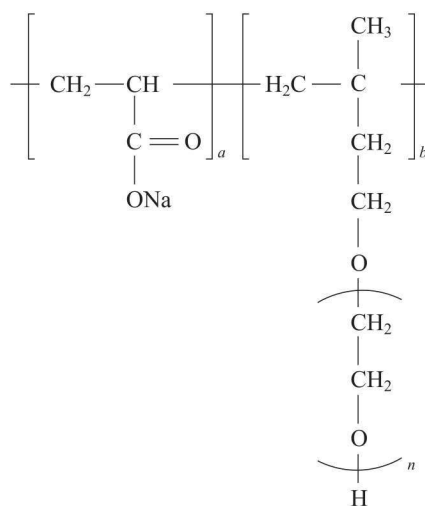


Fig. 1 Chemical structure of the isoprenyl oxy poly(ethylene glycol) (IPEG) based PCE superplasticizer used in the study.

Table 1 Molecular properties and specific anionic charge density of the IPEG PCE sample.

$M_w/$ ($g \cdot mol^{-1}$)	$M_n/$ ($g \cdot mol^{-1}$)	PDI (M_w/M_n)	Specific anionic charge amount at pH 11.7/($\mu eq \cdot g^{-1}$)
35 100	15 700	2.2	2 750

2.2 Preparation and characterization of C – S – H

C – S – H and the C – S – H – PCE nanocomposites were prepared by the co – precipitation method. Aqueous $Ca(NO_3)_2$ and Na_2SiO_3 solutions were combined in water or IPEG – PCE solution to obtain either pure C – S – H or the C – S – H – PCE nanocomposites. The initial molar ratio of CaO/SiO_2 based on the starting materials was 1.0. Two different PCE concentrations, namely 2.7% and 6.7%, were used in the synthesis. First, 0.35 g or 0.90 g of the IPEG – PCE solutions were diluted with 5 mL of water resulting in 2.7% or 6.7% PCE solutions, respectively, which were adjusted to $pH = 8.5 \pm 0.1$ by using aqueous 30% NaOH. Next, solutions of 0.35 g (1.5 mmol) of $Ca(NO_3)_2 \cdot 4H_2O$ dissolved in 5 mL of water and 0.32 g (1.5 mmol) of $Na_2SiO_3 \cdot 5H_2O$ in 5 mL of water were prepared at room temperature. After that, both solutions were added to water or the PCE solution within 5 seconds while stirring at 20 °C. Morphologies of the resulting C – S – H and C – S – H – PCE respectively were observed over time after 5 min, 15 min, 1 h, 2 h, 4 h, 24 h and 48 h via TEM microscopy.

TEM micrographs of the C – S – H and the C – S – H – PCE samples were collected on a JEOL JEM 2011 instrument (JEOL, Japan) equipped with a LaB_6 cathode. Isopropanol suspensions of the C – S – H samples as prepared were placed on a 300 mesh Cu grid with carbon support films (Quantifoil Micro Tools GmbH, Germany) with a plasma – treated surface.

Powder X – ray diffraction (XRD) patterns were obtained from a BRUKER AXS D8 diffractometer (Karlsruhe, Germany) with *Bragg – Brentano* geometry working at 30 kV and 35 mA with $Cu K\alpha$ radiation between 4.0° and $60^\circ 2\theta$.

The silicate species present in the synthesized C – S – H and C – S – H – PCE nanocomposites was characterized by ^{29}Si MAS NMR spectroscopy using a Bruker Avance 300 MHz instrument operating at a resonance frequency of 59.595 MHz. The powder samples were filled into a 7 mm zirconia rotor and spun at 5 kHz. All spectra were recorded with a relaxation delay of 45 s, and tetrakis (trimethylsilyl) silane was used as external standard.

3 Results and Discussion

3.1 Initial nucleation of C – S – H

The early nucleation and crystallization of C – S – H synthesized from aqueous solutions of $Ca(NO_3)_2$ and Na_2SiO_3 in the absence and presence of an IPEG – PCE copolymer was observed via TEM imaging. After 5 minutes of reaction (Fig. 2), pure C – S – H as well as C – S – H – PCE

particles exhibit globular morphology, with diameters in the range of 40 – 60 nm. Most interestingly, a thin layer surrounding the C – S – H droplets was observed on the C – S – H – PCE precipitates, resulting in a core – shell structure (Fig. 3). The layer thickness of the C – S – H particles precipitated at low concentration of the IPEG – PCE solution (2.7%) was found at 3 – 4 nm (Fig. 3 (b)) while at high PCE concentration (6.7%), the thickness of the PCE shell was determined at 6 – 8 nm (Fig. 3 (c)).

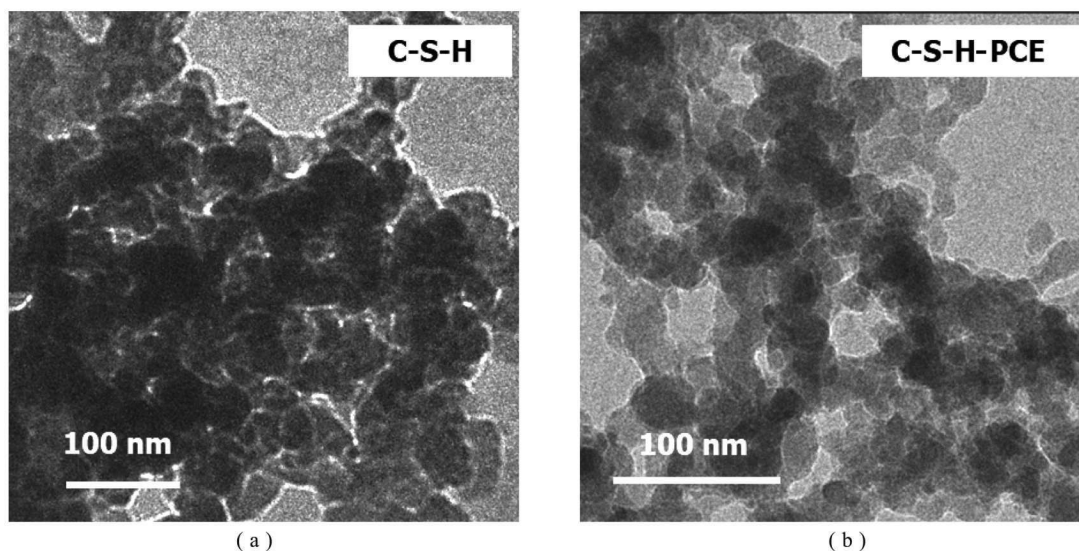


Fig. 2 TEM images of C – S – H (a) and C – S – H – PCE (b) precipitates after 5 min of ageing.

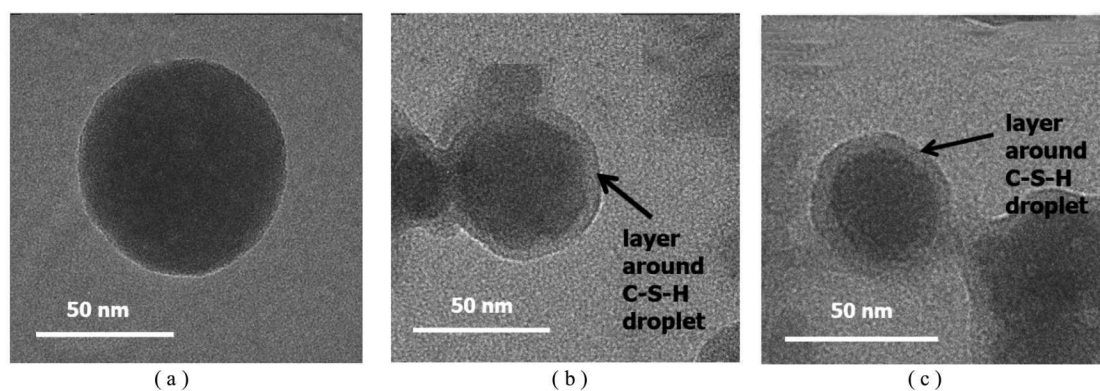


Fig. 3 High resolution TEM images of C – S – H droplets formed in (a) the absence and presence of an IPEG – PCE polymer at (b) 2.7% and (c) 6.7% .

(a) C – S – H; (b) C – S – H – PCE 2.7% ; (c) C – S – H – PCE 6.7%

3.2 Conversion of C – S – H globules to nanofibils

Appearance of the initially globular C – S – H and C – S – H – PCE precursors was monitored

over time via TEM imaging. For the pure C – S – H, the transformation from globular to foil – like morphology had already started 15 minutes after the $\text{Ca}(\text{NO}_3)_2/\text{Na}_2\text{SiO}_3$ solutions had been combined. After 1 hour, the C – S – H globules had completely disappeared while a network of C – S – H nanofoils with lengths of ~ 150 nm and a thickness of ~ 5 nm was found (Fig. 4).

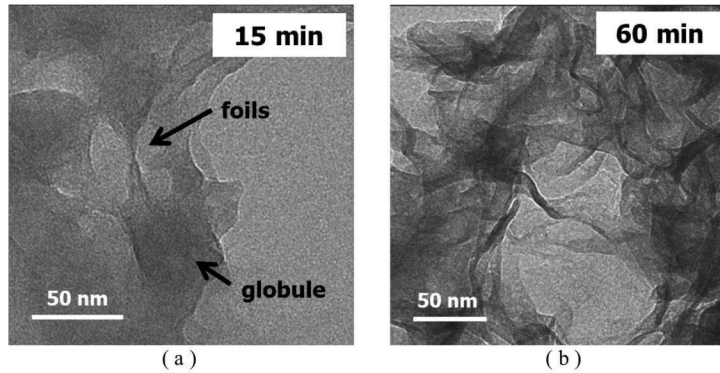


Fig. 4 TEM images of C – S – H particles after 15 (a) and 60 min (b) of crystallization.

However, TEM imaging of the C – S – H – PCE precipitates revealed a delayed transformation from the initial globules to the nanofoils. At low PCE concentration (2.7%), beginning conversion was evidenced after 2 h by the appearance of first needle – like C – S – H crystallites. Furthermore, after 4 h the globules had completely transformed into nanofoils (Fig. 5 (a)). At high PCE concentration (6.7%), a strongly delayed conversion from the C – S – H globules to the nanofoils was observed (Fig. 5 (b)). Even after 4 h, still only C – S – H – PCE globules were present while after 48 h of ageing a mixture of globules and foils with lengths of 30 – 50 nm (and thus much smaller than for pure C – S – H) were found. This effect presumably is owed to a higher amount of PCE adsorbed which leads to a thicker polymer layer on the C – S – H particles.

The results suggest that, following a non – classical nucleation mechanism, early on C – S – H is formed as a metastable droplet which then transforms to the thermodynamically more stable, foil – like morphology. The IPEG – PCE delays the conversion to the nanofoils significantly.

3.3 Structure of early C – S – H

The XRD patterns of pure C – S – H synthesized at various ageing times are shown in Fig. 6. Immediately after precipitation and nucleation (0 and 5 min), a broad peak indicating a highly disordered structure was detected, suggesting amorphous character. While at 60 min of ageing, the diffraction pattern of semi – crystalline C – S – H (I) constituting an imperfect version of 1.4 nm tobermorite was clearly observed. The main $hk0$ reflections (100, 110, 200, 020) appear at 16.7° , 29.0° , 31.9° and $49.7^\circ 2\theta$, respectively. Moreover, the 002 reflection can be found at $7.2^\circ 2\theta$ which signifies a d spacing between the silicate layers of 1.24 nm.

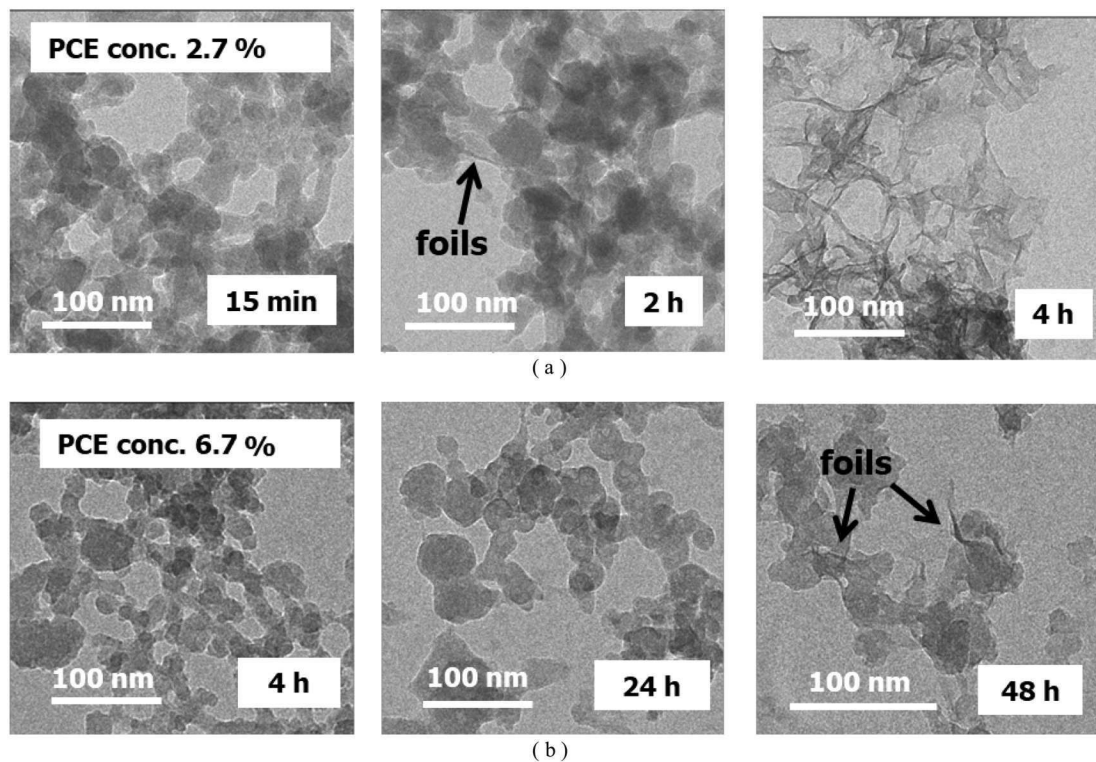


Fig. 5 TEM images of C-S-H precipitated in the presence of an IPEG-PCE polymer at 2.7% (a) and 6.7% (b) concentration at various ageing times.

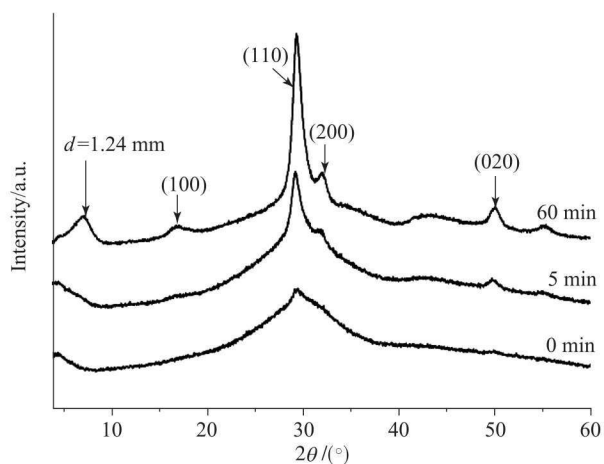


Fig. 6 XRD patterns of synthesized pure C-S-H obtained at 0, 5 and 60 min of crystallization, respectively.

The ^{29}Si MAS NMR spectra of pure C-S-H obtained from the precipitation are shown in Fig. 7. At very early crystallization of 0 and 5 min, the spectra show a broad peak characteristic for end-chain (Q^1 , $\delta = -79$ ppm), chain member (Q^2 , $\delta = -85$ ppm) and branching site (Q^3 , $\delta = -93$ ppm) silica tetrahedra. However, after 60 minutes of ageing, the branching units have

disappeared, suggesting that only linear silicate chains are present in the C - S - H nanofoils. This result supports that the C - S - H globules obtained at very early crystallization exhibit branched silicate chains while the C - S - H nanofoils resulting from the conversion of the globules showed only linear silicate chains.

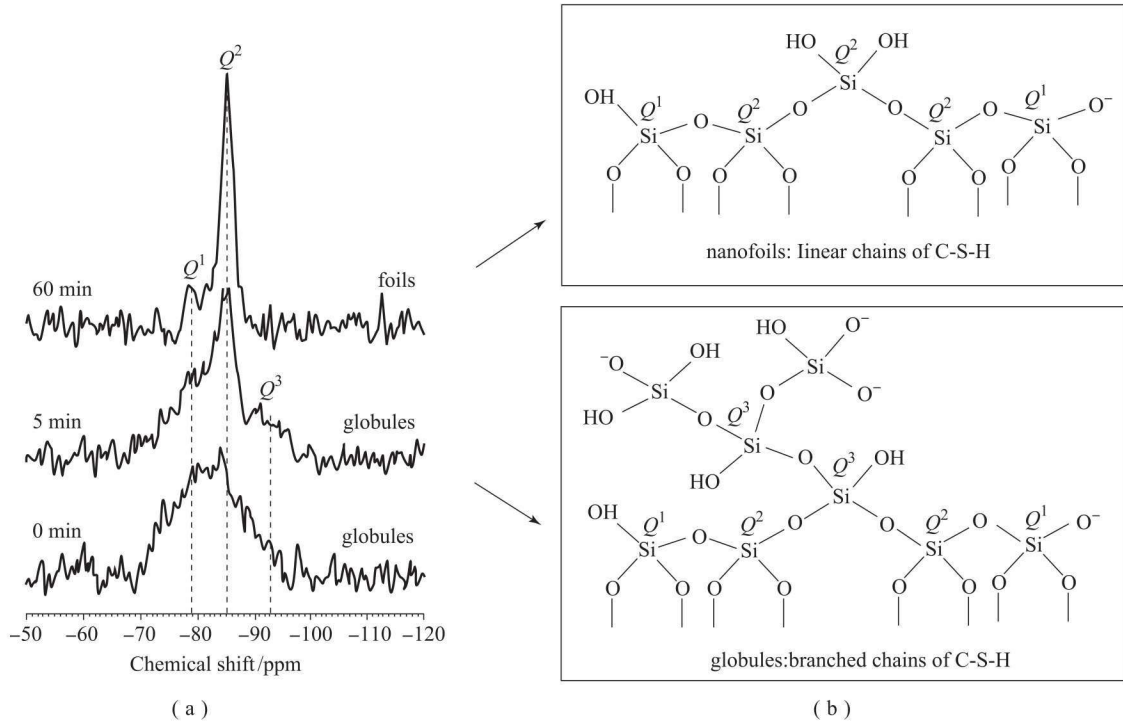


Fig. 7 ^{29}Si MAS NMR spectra of pure C - S - H precipitates obtained at 0, 5 and 60 min of ageing
 (a) and illustration of structural model of linear and branched silicate chains
 (b) present in the globular C - S - H particles and the C - S - H foils, respectively.

4 CONCLUSION

The initial nucleation and crystallization of C - S - H prepared by co - precipitation from $\text{Ca}(\text{NO}_3)_2$ and Na_2SiO_3 in the absence and presence of an IPEG - PCE superplasticizer was studied. It was found that initially a metastable precursor of C - S - H presenting globular morphology is formed which later converts to the C - S - H nanofoils following a non - classical nucleation mechanism. The presence of the PCE delays the conversion from globular to nanofoil - like C - S - H for several hours because of a layer surrounding the globules which presumably consists of PCE polymer. At high PCE concentration, transformation to the C - S - H nanofoils is strongly delayed for several days due to the thicker layer of adsorbed PCE polymer coating the globular C - S - H particles.

The globular precursor of C - S - H exhibits a highly disordered structure containing branched

silicate chains. Whereas the C-S-H foils formed after the conversion show a layer structure of semi-crystalline C-S-H containing non-branched silicate chains.

REFERENCES

- [1] Scrivener K, Nonat A. Hydration of cementitious materials, present and future [J]. Cement and Concrete Research, 2011 (41): 651-665.
- [2] Richardson I G. The Nature of C-S-H in Hardened Cements [J]. Cement and Concrete Research, 1999 (29): 1131-1147.
- [3] Taylor H F W. Cement Chemistry [M]. 2nd ed. London: Thomas Telford Publishing, 1997: 142-159.
- [4] Cölfen H, Antonietti M. Mesocrystals and Nonclassical Crystallization [M]. Chichester: John Wiley & Sons, Ltd., 2008: 7-50.
- [5] Rieger J, Frechen T, Cox G, Heckmann W, Schmidt C, Thieme J. Precursor Structures in the Crystallization/Precipitation Processes of CaCO_3 and Control of Particle Formation by Polyelectrolytes [J]. Faraday Discuss, 2007 (136): 265-277.
- [6] De Yoreo J J, Gilbert P U P A, Sommerdijk N A J M, Penn R L, Whitlam S, Joester D, Zhang H, Rimer J D, Navrotsky A, Banfield J F, Wallace A F, Michel F M, Meldrum F C, Cölfen H, Dove P M. Crystallization by Particle Attachment in Synthetic, Biogenic, and Geologic Environments [J]. Science, 2015 (349): 6247-6256.
- [7] Uchikawa H, Hanchara S, Sawaki D. The Role of Steric Repulsion Force in the Dispersion of Cement Particles in Fresh Paste Prepared with Organic Admixture. Cement and Concrete Research, 1999, 27 (1): 37-50.
- [8] Yoshioka K, Sakai E, Daimon M, Kitahara A. Role of Steric Hindrance in the Performance of Superplasticizers for Concrete [J]. Journal of the American Ceramic Society, 1997; 80 (10): 2667-2671.
- [9] Plank J, Hirsch C. Superplasticizer Adsorption on Synthetic Ettringite [R]. In: Seventh CANMET/ACI Conference on Superplasticizers in Concrete. Berlin: ACI, 2003: 283-298.
- [10] Nicoleau L, Gädt T, Chitu L, Maier G, Paris O. Oriented Aggregation of Calcium Silicate Hydrate Platelets by the Use of Comb-like Copolymer [J]. Soft Matter, 2013 (9): 4864-4874.
- [11] Kanchanason V, Plank J. Role of pH on the Structure, Composition and Morphology of C-S-H-PCE Nanocomposites and their Effect on Early Strength Development of Portland Cement [J]. Cement and Concrete Research, 2017 (102): 90-98.
- [12] Kanchanason V, Plank J. Effectiveness of a Calcium Silicate Hydrate-Polycarboxylate Ether (C-S-H-PCE) Nanocomposite on Early Strength Development of Fly Ash Cement [J]. Construction and Building Materials, 2017, accepted.